Evaluating spatiotemporal patterns of arsenic, antimony, and lead deposition from legacy gold mine emissions using lake sediment records

Article *in* Applied Geochemistry · July 2021

DOI: 10.1016/j.apgeochem.2021.105053

Izabela Jasiak
Hatch Ltd.

Johan A. Wiklund
University of Waterloo

Raoul-Marie Couture
Laval University

Roland I. Hall
University of Waterloo

Journal Pre-proof

Evaluating spatiotemporal patterns of arsenic, antimony, and lead deposition from legacy gold mine emissions using lake sediment records

Izabela Jasiak, J.A. Wiklund, E. Leclerc, J.V. Telford, R.M. Couture, J.J. Venkiteswaran, R.I. Hall, B.B. Wolfe

PII: S0883-2927(21)00184-0

DOI: https://doi.org/10.1016/j.apgeochem.2021.105053

Reference: AG 105053

To appear in: *Applied Geochemistry*

Received Date: 10 March 2021

Revised Date: 27 June 2021

Accepted Date: 10 July 2021

Please cite this article as: Jasiak, I., Wiklund, J.A., Leclerc, E., Telford, J.V., Couture, R.M., Venkiteswaran, J.J., Hall, R.I., Wolfe, B.B., Evaluating spatiotemporal patterns of arsenic, antimony, and lead deposition from legacy gold mine emissions using lake sediment records, *Applied Geochemistry*, https://doi.org/10.1016/j.apgeochem.2021.105053.

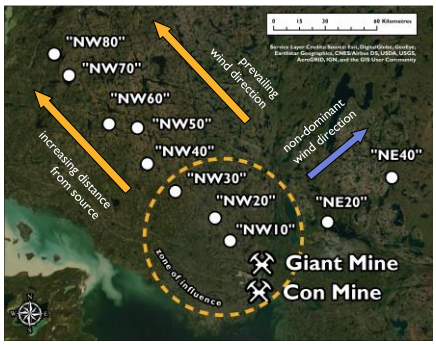

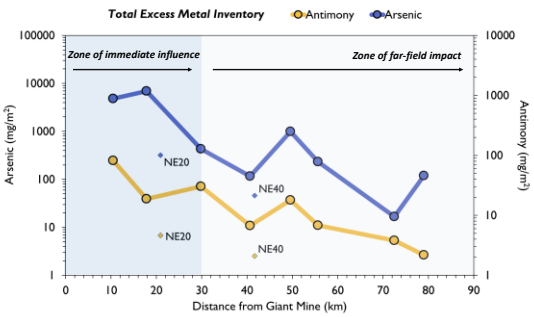

Evaluating spatiotemporal patterns of arsenic, antimony, and lead deposition from legacy gold mine emissions using lake sediment records

Jasiak[1*], Izabela, J.A. Wiklund[1], E. Leclerc[2], J.V. Telford[1,3], R.M. Couture[2], J.J. Venkiteswaran[3], R.I. Hall[1], B.B. Wolfe[3]

[1]Department of Biology, University of Waterloo, Waterloo, ON, Canada
[2]Département de Chimie, Université Laval & Centre d'études Nordiques, Québec, QC, Canada
[3]Department of Geography and Environmental Studies, Wilfrid Laurier University, Waterloo, ON, Canada

*Corresponding Author: ijasiak@uwaterloo.ca

Submitted to Applied Geochemistry on March 10th, 2021

Revised: June 22, 2021

Author Contributions

Izabela Jasiak, Department of Biology, University of Waterloo, Waterloo, ON – *formal analysis, investigation, data collection, writing*

Johan A. Wiklund, Department of Biology, University of Waterloo, Waterloo, ON – *formal analysis, investigation*

Emilie Leclerc, Département de Chimie, Université Laval & Centre d'études Nordiques, Quebec City, QC – *data collection, investigation*

James V. Telford, Department of Geography and Environmental Studies, Wilfrid Laurier University, Waterloo, ON – *data collection, conceptualization*

Raoul M. Couture, Département de Chimie, Université Laval & Centre d'études Nordiques, Quebec City, QC – *conceptualization, funding acquisition*

Jason J. Venkiteswaran, Department of Geography and Environmental Studies, Wilfrid Laurier University, Waterloo, ON – *conceptualization, funding acquisition*

Roland I. Hall, Department of Biology, University of Waterloo, Waterloo, ON – *conceptualization, writing, review and editing, supervision, funding acquisition*

Brent B. Wolfe, Department of Geography and Environmental Studies, Wilfrid Laurier University, Waterloo, ON – *conceptualization, writing, review and editing, supervision, funding acquisition*

Abstract

Gold mining operations near Yellowknife (Northwest Territories, Canada) released vast quantities of arsenic trioxide during the 1950s, which dispersed across the landscape. Contemporary measurements of arsenic concentrations in lake water and surficial sediment identify enrichment within a 30 km radius. However, paleolimnological studies have identified possible evidence of mining influence during the 1950s at a lake beyond this distance, suggesting a more expansive legacy footprint may exist. Here, we analyze spatiotemporal patterns of arsenic, antimony, and lead deposition from sediment cores at lakes located 10-40 km (near-field) and 50-80 km (far-field) from the mines along the prevailing northwesterly wind direction (NW) and 20-40 km to the northeast (NE) of the mines to improve characterization of the legacy footprint of emissions. We build upon previous findings to determine if: 1) there is evidence of mine-related pollutants beyond the well-established 30 km radius and 2) enrichment is greatest in the prevailing wind direction, as expected for aerial dispersion from a point source of emissions. Results demonstrate enrichment since the 1950s for arsenic and antimony at least as far as 80 km to the NW and 40 km to the NE, thus legacy deposition extended beyond the currently defined 30 km radius 'zone of immediate influence'. Concentrations, enrichment factors, and total excess inventories of arsenic and antimony decline with distance from the mines and are greater along the prevailing (NW) than orthogonal (NE) wind direction. Peak concentrations in uppermost sediment strata at near-field lakes in the prevailing wind direction suggest supply of arsenic and antimony remains high from legacy stores in the catchment and lake sediment profiles >60 years after emissions were released. Such lasting influence of legacy emissions likely is not limited to mines in the Yellowknife region, and paleolimnological approaches can effectively delineate zones of past and ongoing pollution from legacy sources elsewhere.

1. Introduction

Geological deposits have provided ample opportunity for mineral exploration in northern Canada (Mudroch et al. 1986, Tenkouano et al. 2019). However, the exploitation of natural resources has often had a profound impact on the environment. In sparsely populated regions, insufficient environmental monitoring prior to, during, and after resource development has complicated the environmental assessment process and, consequently, natural or pre-industrial conditions in these regions remain largely unknown (Thevenon et al. 2011, Gawel et al. 2014, Birch 2017, Klemt et al. 2020). As a result, it remains challenging to evaluate the extent and persistence of mine-related pollutants in remote regions.

Geochemical exploration, in particular the pursuit of gold, has provided opportunity for large-scale investigations of mining impacts (Grosboi et al. 2011, Keshavarzi et al. 2012, Morra et al. 2015, Cai et al. 2017, Kinimo et al. 2018). In the Northwest Territories, Canada, the history of mining includes a legacy of pollution from two major mines: Giant Yellowknife Gold Mines Ltd. (Giant Mine) located ~ 5 km north of Yellowknife and the Consolidated Mining and Smelting Company (Con Mine) ~ 2 km south of Yellowknife (Indian and Northern Affairs Canada 2007, Government of Canada 2014a). At the Giant Mine deposit, gold is hosted primarily in arsenopyrite and required roasting (500°C) to create iron oxides amendable to cyanidation (Hocking et al. 1978, Walker et al. 2005; 2015, Fawcett et al. 2015). As by-products of the oxidation process, arsenic trioxide (As_2O_3) and sulfur dioxide (SO_2) were released from the roaster stack and deposited onto the landscape in the Yellowknife region (Hutchinson et al. 1982). Between 1948 and 1999, more than 20,000 tonnes of As_2O_3 were emitted into the atmosphere, the large majority of which were released from Giant Mine during its first three years of operations (1949-1951) (Hocking et al. 1978, Indian and Northern Affairs Canada 2007, Sandlos and Keeling 2012, Jamieson 2014, Galloway et al. 2015). Emissions gradually decreased during the next ten years with the introduction of pollution abatement and additional gold recovery measures. Most effective was a baghouse dust collector installed in 1958 (Hocking et al. 1978, Government of Canada 2014b).

A lack of effective emission controls prior to 1951 resulted in the widespread contamination of lakes, rivers, vegetation, and soils in the Yellowknife region, where the environmental changes have been well documented (Wagemann et al. 1978, Hutchinson et al. 1982, Fawcett et al. 2015, Palmer et al. 2015; 2021, Thienpont et al. 2016, Houben et al. 2016, Jamieson et al. 2017, Schuh et al. 2018; 2019, Galloway et al. 2018, Cheney et al. 2020, Pelletier et al. 2020). Arsenic remains an element of concern in the region due to links with increased risks of cancer and respiratory issues in humans (Ng and Gomez-Caminero 2001). Arsenic can also affect the growth and reproductive habits of fish species (Boyle et al. 2008, de Rosemond et al. 2008, Erickson et al. 2010, Cott et al. 2016, Chetelat et al. 2019). Lakes located downwind of the mines have received the greatest deposition of legacy pollution (Galloway et al. 2012; 2015, Jamieson 2014, Palmer et al. 2015, Schuh et al. 2018, Van Den Berghe et al. 2018, Cheney et al. 2020). Studies thus far have delineated a 30 km radius ‘zone of immediate influence’ or equivalent ‘zone of probable influence’ (hereafter referred to as the former) from the mines based mainly on measurements of recently-deposited surficial bottom sediment and surface water of lakes (Galloway et al. 2012; 2015; 2018, Palmer et al. 2015). Thus, past studies have primarily assessed present-day conditions, which may not represent the extent of the dispersal of legacy emissions during the 1950s. More recently, a paleolimnological investigation by Cheney et al. (2020) identified that arsenic enrichment during the period of peak emissions can be detected at least as far as 40 km from the mines during the period of peak emissions. While their study intended on using lakes east and northeast of the mines as unimpacted reference lakes, measurable increases in sediment arsenic concentrations during peak emission release suggested otherwise (Cheney et al. 2020). Additionally, a paleolimnological study by MacDonald et al. (2016) in the Slave River Delta, over 140 km southeast of the mines, identified elevated arsenic concentrations (~ 20 mg/kg) during the 1950s. Collectively, these findings suggest that the dispersal of legacy pollution from Giant and Con mines during the 1950s is not yet fully understood.

While lake sediment profiles preserve a temporal record of pollutant deposition (Smol 2008, Birch 2017), interpretation of stratigraphic variation in arsenic concentration requires an understanding of the complex

processes that may influence its deposition and stability within the sediment column (Outridge and Wang 2015). Depending on redox conditions, oxide-bound arsenic can dissolve into sediment porewater, mobilize upwards and/or downwards through the sediment column, and be released into overlying surface waters (Smedley and Kinniburgh 2002, Couture et al. 2008, Palmer et al. 2019). Mining-derived arsenic concentrations in sediment can be compared to less mobile elements also present in the mined ore that were released into the environment during processing. Antimony is much less mobile in lake sediments than arsenic (Fawcett et al. 2015) and is also present in the ore at Giant Mine (SRK Consulting Engineers and Scientists 2002). Thus, antimony has been used in lake sediment studies in conjunction with arsenic to support identification of mining influence (Houben et al. 2016, Schuh et al. 2018, Palmer et al. 2019). Lead concentrations can also be elevated in mining-impacted sediments (Thienpont et al. 2016, Chetelat et al. 2017, Cheney et al. 2020, Pelletier et al. 2020); as this element is not considered to be mobile in lake sediments, it can similarly be used as a tracer of primary mining-derived arsenic deposition in the absence of detailed analysis of mineralogy (Gallon et al. 2004).

Here, we evaluate the degree of contamination beyond the 30 km 'zone of immediate influence' from Giant and Con mines (Hocking et al. 1978, Wagemann et al. 1978, Hutchinson et al. 1982, Galloway et al. 2012; 2015, Palmer et al. 2015, Houben et al. 2016, Galloway et al. 2018). We employ a paleolimnological approach to quantify the deposition of mining-associated metal(loids) arsenic, antimony, and lead (herein referred to as metals) from Giant and Con Mine emissions along two transects, one in the dominant wind direction to the northwest and the other in the less frequent wind direction to the northeast (based on data from 1971-2000 in Galloway et al. 2018 and Government of Canada 2019). Arsenic, antimony, and lead concentrations from ten radiometrically-dated sediment cores are used to assess if: 1) there is evidence of deposition of arsenic, antimony, and lead from Giant and Con mines dispersing beyond the previously determined 30 km radius; 2) spatiotemporal patterns, degree of enrichment, and excess inventories for arsenic and antimony differ with respect to wind direction; 3) surficial sediments of near- and far-field (>40 km) lakes continue to receive pollution from legacy stores

in the catchment and upward mobility from deeper lake sediments. This study provides new data that expands upon the current understanding of the area affected by legacy emissions from Giant and Con mines. Approaches and findings can be used to guide future research here and elsewhere towards determining the fate of legacy stores of mining-sourced metals within catchments and lake sediment profiles.

2. Methods

2.1. Study location

The study area lies within the traditional territory of the Dene (Yellowknives Dene First Nation, Tłı̨chǫ Dene; Government of Northwest Territories n.d.) within Canada's Taiga Shield (Ecosystem Classification Group 2008). Lakes selected for this study range in size (0.08-2.72 km^2; average area: 1.0 km^2) and water depth (1.5-24 m; average depth: 6.96 m) and are located at roughly 10 (northwest) and 20 (northeast) km increments from Giant Mine (Table 1; Figure 1). In this study, lakes are grouped into three categories: northwest near-field (NW10-40), northwest far-field (NW50-80), and northeast (NE20, NE40) and are referenced with respect to distance in kilometers from Giant Mine. Near-field lakes are mainly found within the previously studied area of mining-derived metal deposition, while far-field lakes exist at distances from the mine site beyond those previously explored from a paleolimnological perspective. Most of the study lakes (NW10, NW20, NW30, NW40, NW50, NW60, NW70) are underlain predominantly by granitic bedrock (Stubley and Irwin 2019) where arsenic concentrations average 2 ppm (Boyle 1960), comparable to the worldwide average for granitic rocks (Turekian and Wedepohl 1961). Lakes NW80, NE20, and NE40 are underlain by sedimentary bedrock dominated by metaturbidites (average As concentration: 2-64 ppm; Boyle 1960).

2.2. Field methods

Sediment core collection

Using a Uwitec gravity corer fitted with PVC tubes (86-mm internal diameter), two sediment cores were collected from the pontoon of a helicopter in a deep-water region of each lake based on depth-finder measurements in June 2018 (NW transect lakes) and June 2019 (NE transect lakes). Sediment cores obtained from lakes along the NW transect were transported back to a field base in Yellowknife and sectioned within 24 hours of retrieval into 0.5 cm intervals, but were later consolidated into 1.0 cm intervals to obtain sufficient sample mass for all laboratory analyses. As a result, NE lake sediments were directly sectioned into 1.0 cm intervals the following year. Sediment samples were then transported to the University of Waterloo where they were stored in the dark at 4°C prior to analysis. Additional sediment cores were collected from the same location at each lake to extract porewater and conduct inverse diagenetic modelling on select metals and are reported in Leclerc et al. (in review).

2.3. Laboratory analyses

2.3.1. Radiometric dating

One core from each lake was subject to radiometric analysis to establish the sediment core chronology. When possible, metals analyses were performed on the same core that was used for dating (NW10, NW30, NW40, NW50, NW60, NE20). To ensure cores at each lake were comparable, loss-on-ignition analyses was performed (Heiri et al. 2001) to compare stratigraphic profiles of organic matter content and instilled confidence in our use of alternate cores for metal analyses at lakes NW20, NW70, NW80 and NE40 where additional sediment was required to complete analyses. Radioisotopes (^{214}Bi, ^{214}Pb, ^{210}Pb, ^{137}Cs) were measured for all intervals between 0 and 25 cm, and at alternating intervals between 25 and 35 cm. For each interval analyzed, 1-2 g of freeze-dried sediment was subsampled and placed into pre-weighed polypropylene tubes to a height of 3.5 cm, sealed with a silicone septum, and 1 cc of 2 Ton Epoxy. One exception to this approach was at lake NW70, where sediment intervals at 0-3 cm, 4-7 cm, and 8-9 cm were combined to obtain sufficient sample mass for analyses in the upper portion of the sediment core. Beyond these depths, sediment was subsampled as described previously and interpolation was used to assign ages to consolidated intervals in the upper portion of the sediment core. After a 21-day

waiting period, which allows for parent and daughter isotopes to reach equilibrium, activity of ^{214}Bi, ^{214}Pb, ^{210}Pb, and ^{137}Cs were measured on an Ortec HPGe Digital Gamma Ray Spectrometer at the University of Waterloo for approximately 3-5 days per sample.

Measurements of total ^{210}Pb activity were corrected for decay since the time of core collection and density using standard methods (Schelske et al. 1994). Using measurements of ^{214}Bi and ^{214}Pb as surrogates for ^{226}Ra, supported ^{210}Pb activity was determined. Unsupported ^{210}Pb (i.e., total ^{210}Pb – supported ^{210}Pb) was determined and used to estimate sediment ages using the Constant Rate of Supply (CRS) model (Binford 1990, Appleby 2001). To supplement the age model based on ^{210}Pb, measurements of ^{137}Cs activity were used to detect a peak associated with above-ground nuclear mass weapon testing in 1963 (Appleby 2001). The dry-mass sedimentation rate was used to extrapolate the sediment chronology beyond the depth where ^{210}Pb background was reached within a core (i.e., where supported ^{210}Pb was equal to total ^{210}Pb).

Focusing factors were determined using ^{210}Pb data and are expressed as a ratio of the measured inventory of unsupported ^{210}Pb within the sediment core to the expected inventory of unsupported ^{210}Pb based on measurement of atmospheric fallout near the study location (Wong et al. 1995, Fuller et al. 1999, Muir et al. 2009, Olid et al. 2010).

2.3.2. Metal concentrations

Concentrations of solid-phase metals in sediment were measured at all lakes and all sediment intervals between 0 and 29 cm. Between 0.25 and 0.50 g (±0.05 g) of freeze-dried sediment was finely ground and homogenized using a mortar and pestle, loaded into pre-weighed plastic tubes, and sent to ALS Laboratories Ltd. (Waterloo, Ontario), a CALA (Canadian Association for Laboratory Accreditation Inc.) certified laboratory, for analysis. Metals were measured after heated digestion with concentrated nitric and hydrochloric acids and using a Collision/Reaction Cell inductively coupled plasma mass spectrometer (CRC ICP-MS) following EPA standard methods 200.2/6020A (ALS Method MET-200.2-CCMS-WT). Certified reference material TILL-2 was used by the analytical laboratory. For samples where 0.50 g

(±0.05 g) of freeze-dried sediment were submitted for analysis, duplicates were analyzed every 5 cm to confirm accuracy of results. Analytical uncertainties, expressed here as the relative percent difference (RPD) between duplicate samples, were reported by ALS Laboratories as: 2.67 % for arsenic (n=15), 5.47 % for antimony (n=14), and 3.85 % for lead (n=15).

2.4. Numerical analyses

2.4.1. Enrichment factors

Enrichment factors (EFs) were used to determine the magnitude of arsenic and antimony enrichment relative to the pre-industrial background. Background concentrations of arsenic and antimony were determined by visual assessment of the stratigraphic profile for individual lakes and metals. Variable concentrations in the sediment record hindered our ability to establish reliable estimates of lead in the pre-industrial era. Furthermore, the possibility of post-depositional mobility of arsenic and antimony within the cores (Couture et al. 2008, Leclerc et al. in review) prevented using a specific pre-industrial time interval for sediment cores from all 10 lakes (e.g., 1935, predating operations of both mines) to establish background concentrations. Therefore, when a metal displayed a near-constant stratigraphic pattern in the lower pre-1935 portion of a sediment core, 'pre-industrial background' was defined as the mean of the concentrations found in the near-constant zone (to 1500 CE). As a result, 20 background concentrations were established across the 10 study lakes for arsenic and antimony and reflect the varying concentrations and post-depositional behaviour of these metals in each sediment core profile. Background estimates were comprised of a minimum of 3 and maximum of 24 samples per lake, depending on the variability in the sediment record. For metals measured in a core from each lake, sediment core depths of background estimates are comparable (within ±4 cm).

Relationships between concentrations of measured metals in sediment at each lake were explored to identify an appropriate lithogenic element for normalization. However, analysis of both arsenic and antimony concentrations to a suite of lithogenic elements identified poor relationships. As a result, lithogenic elements were not appropriate to use as a normalizing agent, despite the recent use of Al, Li,

and Ti by other studies in the Yellowknife region (Sivarajah et al. 2019, Cheney et al. 2020) and in other regions where EFs have been computed from sediment profiles (e.g., Wiklund et al. 2012, Kay et al. 2020). Instead, raw metal concentrations are used in the following equation to compute EF values for each sediment interval:

$$EF = \frac{M_x}{(M_{pre-industrial})}$$

where: M_x is the concentration of a given metal at the interval at x cm depth in a core, and $M_{pre-industrial}$ is the average of the full range of concentrations in the pre-industrial era (to 1500 CE) for a given element.

Here, we adopt criteria of Birch (2017) for classification of enrichment factors. Metals are considered enriched when an EF is ≥1.5 times the pre-industrial background concentration. Metal concentrations with an EF less than 1.5 are considered representative of natural or 'pristine' conditions. EF values ranging from 1.5-3 are classified as minimal enrichment, 3-5 are classified as moderate enrichment, 5-10 are classified as considerable enrichment, and >10 are classified as severe enrichment.

2.4.2. Excess flux and total excess inventory calculations

The contribution of anthropogenic sources of arsenic and antimony deposition to the lake sediments was estimated as the excess flux. Calculation of excess flux involved two steps. First, enrichment factors were multiplied by element concentrations and dry mass sedimentation rates (kg/m^2/year) to determine rates of element flux ($\mathcal{F}$) in units of mg/m^2/year, using the equation (Whitmore et al. 2008, Gomes et al. 2009, Wiklund et al. 2017):

$$\mathcal{F} = \frac{\left[\left(\frac{EF_x - 1}{EF_x}\right) \times SR_x \times C_x\right]}{ff}$$

where: EF_x is the enrichment factor for a given element at interval x,

SR_x is the sedimentation rate in kg/m^2/year at interval x,

C_x is the concentration of the element at interval x, and

ff is the ^{210}Pb-based focusing factor for a given lake.

Second, we calculated the inventory of excess flux ($\mathcal{FI}$) of each metal, which is suggested to provide more accurate estimates of metal fluxes (Bacardit et al. 2012, Wiklund et al. 2020), as:

$$\mathcal{FI} = (A_w - A_x) \times \mathcal{F}_x$$

where: A_w is the age of the sediment interval w,

A_x is the age of the sediment interval x, and

$\mathcal{F}_x$ is the rate of flux (mg/m^2/year) at sediment interval x.

To account for lateral redistribution of sediment across the lake basin due to wind and wave action and changes in basin slope, excess flux inventories were corrected for sediment focusing and adjusted using focusing factors. Focusing factors >1 suggest that metal fluxes have been overestimated while focusing factors <1 suggest metal fluxes have been underestimated. By dividing the total excess flux inventory of a metal at a lake by the focusing factor, the flux was then re-expressed as either greater or smaller than the calculated value. Excess flux inventories for all sediment intervals for each lake were then summed and expressed as the total mass and are representative of the total excess inventory of arsenic and antimony.

3. Results

3.1. Sediment core chronologies

Total ^{210}Pb activity profiles varied among lakes (Figure 2). Activity of ^{210}Pb ranged between 0.01 Bq/g and 1.7 Bq/g overall. Stratigraphic profiles of ^{210}Pb activity were similar at lakes NW10, NW20, and NW60, where activity decreased monotonically with increasing depth. In contrast, ^{210}Pb activity was near-constant or declined at the tops of cores from lakes NW30, NW40, NW50, NW70, NW80, NE20 and NE40 before declining down-core between 2 and 12 cm depth. The depths at which background ^{210}Pb activity was obtained also varied. Most commonly, background ^{210}Pb activity was reached between 6 and 15 cm in depth (NW10, NW20, NW30, NW40, NW50, NE20). At NW60, NW70 and NW80, however, unsupported ^{210}Pb activity persisted to greater depth, and as deep as 29 cm at NE40. Background ^{210}Pb activity ranged between 0.01 and 0.13 Bq/g. Rates of sedimentation varied by an order of magnitude (0.0016 at NW40 to 0.0156 g/cm^2/year at NW80).

Based on results from CRS modelling of the ^{210}Pb profiles, sediment deposited during the 1950s occurred in the upper 5-10 cm of cores from the study lakes, with the exception of NW70 (13 cm), NW80 (15 cm), NE20 (11 cm), and NE40 (15 cm; Figure 2). An increase in ^{137}Cs activity was observed at most lakes (NW40, NW50, NW60, NE20, and NE40) in sediment intervals younger than the 1950s based on ^{210}Pb dating, which is consistent with the record of above-ground nuclear weapon testing (Appleby 2001). The lake sediment cores encompassed a wide range of ages from 207 years to as much as 3220 years (average: 807 years). However, the sediment core from lake NW70 (~ 3220 years old) revealed a sharp change from organic-rich material in the upper 20 cm (~ 1750 CE) to clay-rich material below that strata, which may have resulted in an overestimation of inferred ages. Given the substantially older basal ages of lakes NW40 (~ 1390 CE at 30 cm depth) and NW70 (~ 900 CE at 30 cm depth), metal concentration data presented herein are limited to sediment deposited since ~ 1500 CE to allow for a more consistent comparison of climatic and environmental conditions that may have influenced stratigraphic metal concentrations among lakes.

3.2. Metal stratigraphic profiles

Broad systematic patterns in stratigraphic variation of arsenic, antimony, and lead concentration are evident among the designated groups of lakes (Figure 3). Arsenic and antimony concentrations were typically highest closest to the mine in NW near-field lakes, followed by NW far-field and NE lakes. Lead concentrations, in contrast, were on average higher at NW far-field lakes, followed by NE lakes and NW near-field lakes. Within 40 km of the mine (near-field), arsenic, antimony, and lead concentrations in most lake sediment core profiles demonstrated a continuous increase towards the top of the core, with maxima in uppermost sediments. Beyond this distance (NW far-field) and for the NE lakes, sediment core profiles identified sub-surface peaks aligning closely with timing of maximum emission from Giant Mine in the 1950s (with the exception of NW80) and were followed by a general decline in metal concentrations. Maximum As concentrations for all sediment cores exceed the CCME Probable Effects Level (PEL) for protection of aquatic life (17.0 µg/g; CCME 1999a), whereas maximum Pb concentrations fall below the CCME PEL (93.1 µg/g; CCME 1999b). The CCME does not report a PEL value for Sb in aquatic sediment. Further details regarding the stratigraphic profiles in individual lake groups are provided below.

The range of concentrations found in sediment profiles of near-field lakes (NW10-40) varied for arsenic (range: 7.8-1040.0 µg/g, median: 26.8 µg/g, antimony (range: 0.1-17.5 µg/g, median: 0.5 µg/g), and lead (range: 0.7-8.9 µg/g, median: 2.8 µg/g) (Figure 3). Maximum arsenic and antimony concentrations were highest at lake NW10 (As: 1040.0 µg/g, Sb: 17.5 µg/g) and decreased with distance from Giant Mine (NW40; As: 33.2 µg/g, Sb: 2.4 µg/g). Maximum lead concentrations were also highest at lake NW10 (17.5 µg/g) but did not display a similar pattern of decline with distance (NW40; 6.1 µg/g vs NW30; 5.6 µg/g). Background values ranged from 7.8 to 27.1 µg/g for arsenic (median: 11.2 µg/g) and 0.1 to 0.5 µg/g for antimony (median: 0.2 µg/g). With the exception of the antimony and lead concentration profiles at NW40, which display peak concentrations that align with maximum emissions in the 1950s, the near-

field stratigraphic profiles for arsenic, antimony and lead increased towards the top of the sediment records and concentrations are highest in the most recently deposited sediments.

At far-field lakes (NW50-80), concentrations of arsenic (range: 3.3-240.0 µg/g, median: 19.1 µg/g), antimony (range: 0-3.8 µg/g, median: 0.3 µg/g), and lead (range: 2.7-17.5 µg/g, median: 5.9 µg/g) similarly spanned a wide range but were overall lower in arsenic and antimony than near-field lakes. Here, highest arsenic and antimony concentrations were found at lake NW50 (As maximum: 240.0 µg/g, median: 15.8 µg/g; Sb maximum: 3.8 µg/g, median: 0.3 µg/g) and decreased with distance from Giant Mine (NW80: As maximum: 31.8 µg/g, median: 13.4 µg/g; Sb maximum: 0.7 µg/g, median: 0.2 µg/g). Lead concentrations were highest at NW50 (maximum: 17.4 µg/g, median: 14.5 µg/g) and exceeded that of all other study lakes. With the exception of NW70 (maximum: 15.7 µg/g, median: 8.9 µg/g), average lead concentrations decreased beyond a distance of 50 km. Background concentrations at far-field lakes ranged from 3.3 to 29.1 µg/g for arsenic (median: 12.1 µg/g) and from 0 (below detection limit) to 0.4 µg/g for antimony (median: 0.2 µg/g). At far-field lakes (NW50-80), arsenic and antimony concentrations reached their maximum at depth and aligned with or post-dated the 1950s, whereas the deposition of lead was more variable over time and only formed a distinctive sub-surface post-emission peak at lake NW60.

NE lakes (NE20, NE40) possessed metal concentrations that were nearly an order of magnitude lower in comparison to NW lakes at the same distances. Metal concentrations for the NE lakes ranged from 2.2 to 135.0 µg/g for arsenic (median: 17.1 µg/g), 0 to 3.5 µg/g for antimony (median: 0.3 µg/g), and 0.8 to 11.3 µg/g for lead (median: 5.0 µg/g). Concentrations of arsenic, antimony, and lead were higher at NE20 (As median: 27.8 µg/g, Sb median: 0.2 µg/g, Pb median: 7.4 µg/g) than at NE40 (As median: 9.0 µg/g, Sb median: 0.4 µg/g, Pb median: 2.5 µg/g). At the NE lakes, background concentrations of arsenic ranged from 2.2 to 27.9 µg/g (median: 18.6 µg/g) and background antimony concentrations ranged from 0 to 0.2 µg/g (median: 0.2 µg/g). Maximum concentration of arsenic, antimony, and lead at NE lakes occurred at depth and aligned with or post-dated the 1950s.

3.3. Enrichment factors

Enrichment factors for the NW near-field lakes (NW10-40) ranged from 1.1 to 62.7 for arsenic (average: 7.0) and 1.2 to 44.8 for antimony (average: 11.1; Figure 4). Based on categories identified by Birch (2017), 8 % of arsenic samples in near-field lakes were pristine, 35 % were minimally enriched, 21 % were moderately enriched, 24 % were considerably enriched, and 10 % were severely enriched (Figure 4). For antimony, 2 % of samples were pristine, 15 % were minimally enriched, 21 % were moderately enriched, 21 % were considerably enriched, and 40 % were severely enriched. There was evidence of enrichment above the pre-industrial baseline (EF >1.5) across all near-field study lakes for both metals in sediments deposited during the period of peak emissions (1950s). Consistent with stratigraphic profiles in near-field lake metal concentration data, the greatest enrichment occurred in the uppermost sediment layer, with the exception of NW40 where antimony enrichment was greatest during the 1950s. While there is a sharp gradient in the degree of arsenic enrichment at near-field lakes with distance from Giant Mine, enrichment of both arsenic and antimony began to occur well before the onset of mining operations at near-field lakes and is evident as early as the 1700s at lake NW20 because of post-depositional mobility downward in the sediment core record (Leclerc et al. in review).

At the NW far-field lakes, arsenic enrichment factors ranged between 0.8 and 15.2 (average: 5.1; Figure 4). Approximately 21 % of samples were identified as pristine, 18 % were minimally enriched, 16 % were moderately enriched, 27 % were considerably enriched, and 18 % were severely enriched. Enrichment of antimony at far-field sites ranged from 1.3 to 24.8 (average: 8.1). For antimony, 3 % of samples were pristine, 21 % were minimally enriched, 10 % were moderately enriched, 33 % were considerably enriched, and 33 % were severely enriched. Three of four far-field lakes became enriched in arsenic during the period of peak mine emissions, and all lakes experienced enrichment in antimony at this time. The greatest degree of arsenic and antimony enrichment occurred during or after (~ 30 years) the introduction of pollution abatement measures. Prior to the 1950s, most lakes appear to have experienced some antimony enrichment (NW50, NW60, NW70) while only NW60 experienced arsenic enrichment.

Enrichment factors for arsenic and antimony in uppermost sediments of the far-field lakes have returned to pre-industrial values.

For the NE lakes, enrichment factors for arsenic ranged from 1.2 to 8.4 (average: 4.2) and 2.0 to 34.5 for antimony (average: 14.7). With regards to arsenic, 7 % of samples were identified as pristine, 17 % were minimally enriched, 41 % were moderately enriched, and 34 % were considerably enriched. There was no evidence of severe arsenic enrichment along the NE transect. For antimony, 7 % of sediment samples were minimally enriched, 3 % were moderately enriched, 18 % were considerably enriched, and 71 % were severely enriched. The greatest degree of arsenic and antimony enrichment aligned with or post-dated the 1950s. After the 1950s, arsenic and antimony enrichment declined. Both NE20 and NE40 appear to have experienced some arsenic and antimony enrichment prior to the onset of gold mining in the region, likely due to post-depositional downward mobility. EF values decline towards the surface of these cores and approach the pre-industrial state (EF of 1). In comparison to NW lakes at equivalent distances (NW20, NW40), the degree of enrichment of arsenic and antimony at NE20 and NE40 was comparable.

3.4. Excess metal inventories

Excess metal inventories demonstrated deposition of anthropogenic arsenic and antimony at all study lakes at least as far as 80 km to the northwest and 40 km to the northeast (Figure 5). Spatial trends of excess inventories of arsenic and antimony were comparable across each of the three groups of lakes and ranged from 17 to 6929 mg/m^2 for arsenic (average: 1404 mg/m^2) and from 2 to 82 mg/m^2 for antimony (average: 18 mg/m^2). The amount of excess inventory at each lake was generally associated with distance from Giant Mine and wind direction and is further described below according to lake group.

The inventory of excess arsenic at NW near-field lakes (average: 3076 mg/m^2) was on average 9 times that of far-field lakes (average: 342 mg/m^2) and at least 16 times that of NE lakes (average: 182 mg/m^2). A similar trend was evident for antimony with near-field lake excess inventories (average: 34 mg/m^2) substantially exceeding both far-field (average: 8 mg/m^2) and NE lake excess inventories (average: 5

mg/m^2). On the NW transect, arsenic excess inventories were greatest at lakes NW10 (4826 mg/mg^2) and NW20 (6929 mg/m^2) and decreased with distance from Giant Mine (NW70: 17 mg/m^2; NW80: 120 mg/m^2), with the exception of NW50 (995 mg/m^2). Apart from lakes NW30 (30 mg/m^2) and NW50 (18 mg/m^2), inventories of excess antimony displayed a similar decline with increasing distance from Giant Mine (NW10: 82 mg/m^2 vs NW80: 2 mg/m^2). On the NE transect, total inventories of excess arsenic decreased markedly from NE20 (318 mg/m^2) to NE40 (46 mg/m^2) and was similarly reflected by inventories of excess antimony (NE20: 7 mg/m^2 vs NE40: 3 mg/m^2). Excess inventory of As at NE20 (318 mg/m^2) was less than 20 times at NW20 (6929 mg/m^2) and less than 2 times at NE40 (46 mg/m^2) compared to NW40 (117 mg/m^2). Transect differences in excess antimony deposition were less pronounced, but NE inventories of antimony (range: 3-7 mg/m^2, average: 5 mg/m^2) were ~ 2-3 times less than at the NW lakes at equivalent distances (range: 7-19 mg/m^2, average: 13 mg/m^2).

4. Discussion

4.1. Delineating the footprint of legacy mining emissions

Stratigraphic records revealed evidence of anthropogenic deposition of arsenic and antimony at all study lakes and were quantified using enrichment factors and total excess metal inventories. The co-deposition and similar stratigraphic patterns of arsenic, antimony, and to a lesser extent lead in sediments reinforces the notion that enrichment of metals in sediments of these lakes are the product of emissions from Giant and Con mines rather than from the chemical weathering of bedrock or some other source. Measurement of dissolved arsenic concentrations in surface waters of lakes of the NW transect reported in Leclerc et al. (in review) are consistent with findings of other researchers in the area and similarly identified a 30 km zone (NW10-30) of ‘immediate influence’ from the mines (Galloway et al. 2012; 2015, Palmer et al. 2015). Yet, maximum concentrations and the enrichment of arsenic and antimony in sediment at lakes beyond 30 km, where preserved at depth, align reasonably well with the operational history of the mines and particularly peak emission release in the 1950s.

At NW far-field and NE lakes, arsenic and antimony concentration profiles are characteristic of an isolated anthropogenic event. Sharp decreases towards the sediment surface in arsenic, antimony, as well as lead may reflect the introduction of pollution abatement measures at Giant Mine. Minor observed 'lags' in the sediment record between peak emission release and the recorded atmospheric deposition of mining-derived metals at NW far-field and NE lakes, such as the timing of peak arsenic, antimony, and lead concentrations at NE20 (~ 1960 CE), are likely explained by a combination of the element's post-depositional mobility due to transport and reactions, uncertainties associated with the age model, and the delayed delivery of metals from the surrounding catchment to the lake bottom (Martin and Pederson 2002). Although determination of the pre-industrial background used as part of enrichment factor and excess inventory calculations was conservative, given that arsenic can undergo post-depositional mobility, it remains possible that concentrations were redistributed through the sediment column and confound estimates of enrichment, particularly at NW20 and NW40 (Leclerc et al. in review). Nonetheless, sediment metals concentration data and excess inventories in this region illustrate a clear signal of Giant and Con mine emissions that dispersed at least as far as 80 km to the northwest and 40 km to the northeast; a conclusion that is supported even without the use of enrichment factors (Figure 3). Furthermore, the same conclusion is drawn from excess As inventories derived after inverse diagenetic modelling of the sediment core records along the northwest transect (Leclerc et al. in review). Based on our results, the degree of enrichment and excess inventories of arsenic and antimony, which we attribute to emissions from Giant and Con mines, have been strongly influenced by two factors: 1) distance from the former Giant Mine roaster stack and 2) wind direction.

The degree of enrichment and excess inventories of arsenic and antimony at each lake generally declined with distance from the mines along both NW and NE transects (Figures 4, 5). Enrichment ranged from minimal to severe during the 1950s and was greatest in NW near-field lakes, followed by NW far-field and NE lakes. This pattern was similarly reflected by excess inventories, with the largest quantity of arsenic and antimony deposited closest to the mines (NW10, NW20, NE20) and the smallest at more

distal locations (NW70, NW80, NE40). Within the three lake groups, similar decreases in degree of enrichment and excess inventories were observed with increasing distance. Minor exceptions to these trends are observed between near- and far-field lake groups and are most evident at lake NW50, which is considerably larger and deeper than all other lakes along the transect (Table 1). With respect to NW near-field lakes and NE lakes, results of our sediment metal analyses are largely in agreement with findings of other researchers. Consistent with studies of contemporary surface water (Palmer et al. 2015, Houben et al. 2016), surficial sediment (Galloway et al. 2012; 2015), and soils (Jamieson et al. 2017, Galloway et al. 2018), solid-phase and dissolved arsenic concentrations were highest closest to Giant Mine. Our near-field results also support the findings of other paleolimnological analyses in the Yellowknife region that have identified widespread contamination from gold mining in the area (Thienpont et al. 2016, Schuh et al. 2018, Van Den Berghe et al. 2018, Cheney et al. 2020). However, past studies have been limited to the near-field region of Yellowknife and the surrounding area and have identified a 'zone of immediate influence' within 5 km (Van Den Berghe et al. 2018), 17 km (Palmer et al. 2015, Houben et al. 2016), 20 km (Sivarajah et al. 2020), 24 km (Pelletier et al. 2020), 30 km (Galloway et al. 2018), and 40 km (Cheney et al. 2020) of Giant Mine. Conversely, NW far-field lake sediment records presented here demonstrate that emissions from the mines are present on the landscape at distances well beyond 40 km and following the 1950s resulted in considerable to severe metal enrichment at least as far as 80 km in the prevailing wind direction.

Lake sediment records on the northwest and northeast transects effectively illustrated that deposition of mining-derived metals was strongly dictated by wind direction, in addition to distance from the mines. Much like the NW far-field lakes, stratigraphic records of NE lakes (NE20, NE40) exhibited sharp increases in all three metals during and shortly after the 1950s with enrichment ranging from moderate (arsenic) to severe (antimony). However, in comparison to lakes in the northwest at the same distances (NW20, NW40), the total inventory of excess arsenic and antimony at NE20 and NE40 was ~ 2-20 times lower. Findings are consistent with studies of Palmer et al. (2015) and Galloway et al. (2018) that

identified lakes downwind along the prevailing wind direction from Giant Mine exhibited the highest dissolved arsenic concentrations in their surface water and surface sediments. However, the presence of excess arsenic and antimony at lakes to the northeast indicates that lakes in the non-dominant wind direction were not exempt from mining emissions and aligns with paleolimnological data reported by Cheney et al. (2020). Additionally, given the mass of arsenic and antimony deposited in excess at NW80, 79 km NW of Giant Mine (As: 120 mg/m^2, Sb: 2 mg/m^2) and NE40, 41 km NE of Giant Mine (As: 46 mg/m^2, Sb: 3 mg/m^2), it is likely that emissions released from Giant and Con mines extended beyond an 80 km NW and 40 km NE radius. These results, as well as arsenic enrichment found in a lake in the Slave River Delta located 140 km southeast of the mines (MacDonald et al. 2016), suggest that atmospheric deposition likely occurred on the landscape beyond these distances and in directions not yet fully explored.

Across all lake sediment records, excess arsenic was an order of magnitude greater than excess antimony. Similar observations were made by Cheney et al. (2020) where lake sediment records in the non-dominant wind direction exhibited smaller increases in antimony in comparison to arsenic. Given that atmospheric residence times of arsenic and antimony have been estimated to be similar (4-10 days and 7-14 days, respectively; Han et al. 2003, Tian et al. 2014, Wai et al. 2016, Herath et al. 2017, Wiklund et al. 2020), such a phenomenon is likely explained by the proportionally smaller release of antimony in comparison to arsenic from the roaster stack (SRK Consulting Engineers and Scientists 2002, Bromstad et al. 2017). Additionally, because lead was released in much smaller quantities than both arsenic and antimony (SRK Consulting Engineers and Scientists 2002) and deposition of lead from fossil fuel combustion in the 1960s was widespread, it is not surprising that the trend of decreasing concentrations with distance is less pronounced for lead than other metals. While it is possible that the Giant and Con mine signal in the lead record has been modified by the introduction and subsequent ban of leaded gasoline in North America (Peter and Wozniak 2001), the comparable depositional history of all three metals at most lakes across the two transects suggests influence of lead from gasoline combustion was minimal.

4.2. Influence of catchment and diagenetic processes on metal stratigraphic profiles

The depositional histories and stratigraphic profiles for arsenic and antimony concentrations varied systematically across the three lake groups. Arsenic and antimony concentrations increased towards the top of the sediment cores at NW near-field lakes, while maximum concentrations occurred at depth at NW far-field and NE lakes, forming distinctive down-core peaks in close agreement with, or post-dating, maximum emissions during the 1950s (Figure 3). There are at least three possible explanations for the differences observed in arsenic and antimony concentration profiles across the three lake groups: 1) ongoing supply from the catchment and within-lake lateral transport of arsenic and antimony is greatest closest to the mine, 2) post-depositional mobility of arsenic and/or antimony has occurred, or 3) a combination of 1) and 2).

Proximity to the mines, which has long been identified as the key determinant for metal enrichment in lakes in the region (e.g., Hocking et al. 1978, Wagemann et al. 1978, Galloway et al. 2012; 2015, Palmer et al. 2015, Jamieson et al. 2017) and demonstrated by results presented here, is likely also a determinant of metal enrichment in the terrestrial environment. Ongoing supply of metals, delivered to the land by aerial mining emissions in the 1950s and subsequently mobilized via catchment erosion, has been identified as a potential explanation for the persistence of metal enrichment in near-surface lake sediments, particularly in the extensively-studied 30 km radius of the mines (Thienpont et al. 2016, Schuh et al. 2018; 2019, Pelletier et al. 2020). A possible mechanism for the rising concentrations is greater runoff and catchment erosion, which may have accelerated under a warming climate and more frequent wildfires (Wang et al. 2015, Abraham et al. 2017, Giesler et al. 2017, Pelletier et al. 2020b). Given that As concentration in the sediment cores does not exhibit relationships with lithogenic elements, we speculate that As delivered by this pathway may be in dissolved form, possibly associated with influx of dissolved organic matter (Audette et al. 2020). Mining-derived metals may also be supplied via lateral movement of sediment from shallow to deep parts of the basin (Schuh et al. 2018; 2019). However, focusing factors of <1 at near-field lakes NW10, NW20, and NW30 (Figure 2) do not support this as a

possible mechanism. In contrast, NW far-field and NE lake catchments may have rapidly exhausted their lesser supplies of terrestrial legacy metals, which allowed for preservation of peak concentrations approximately contemporaneous to peak emissions in these stratigraphic records. Despite being located at distances equivalent to near-field lakes NW20 and NW40, northeast lakes NE20 and NE40 may have similarly exhausted their comparatively smaller terrestrial supply of legacy metals because of lower supply of pollutants to the landscape in non-dominant wind directions. Mining-derived metals at the sediment surface were also identified by Schuh et al. (2018) in lakes ~ 5 km from Giant Mine and were determined to be due in part to terrestrial loading from the surrounding catchment. Southwest of the mine in Yellowknife Bay, legacy metals (particularly lead) have similarly accumulated at the sediment surface and are likely to have originated from the terrestrial environment or other regions of the Bay (Pelletier et al. 2020).

Mobility of arsenic, and to a lesser extent antimony, in lake sediments has been well documented (Mudroch et al. 1989, Martin and Pederson 2002, Smedley and Kinniburgh 2002, Couture et al. 2010, Fawcett et al. 2015, Van Den Berghe et al. 2018, Miller et al. 2019). However, given that lead is considered immobile in lake sediments (Outridge and Wang 2015, Thienpont et al. 2016, Pelletier et al. 2020) and was also emitted from the Giant Mine roaster, we can use the similarities and differences among the three metals to gauge the influence of post-depositional mobility on the stratigraphic profiles. For example, the parallel concentrations of arsenic, antimony, and lead at NW10-30 suggests that post-depositional mobility is unlikely to have been a dominant cause of enrichment present in uppermost strata. In contrast, at NW40, where trends of arsenic concentrations were consistent with those observed at lakes NW10-30 (NW40 maximum: 0-1 cm, ~ 2016), the antimony record formed a distinctive down-core peak in ~ 1960 (maximum: 2.35 ug/g, 5-6 cm) and behaved more similarly to NW far-field and NE lakes. Given its relatively immobile nature in comparison to its more mobile co-pollutants, the lead record at NW40 (maximum: 7.06 ug/g, 5-6 cm) suggests that maximum arsenic concentrations found at the sediment surface are the product of post-depositional mobility. Similar inferences can be drawn from lake

NW20 where a deviation from the lead record by its otherwise parallel co-pollutants (arsenic, antimony) may indicate post-depositional mobility has occurred. Our inferences of post-depositional arsenic mobility in the stratigraphic records at NW20 and NW40 agree with reconstructions of diagenetic processes over time via inverse reactive transport modelling (Leclerc et al. in review). For shallow lakes in the region that become anoxic in winter, seasonal development of low oxygen concentration promotes perpetual reductive dissolution of As that can lead to surface-sediment enrichment (Palmer et al. 2019), which may be playing a role here, particularly at lakes NW20 and NW40. Additional research could determine the influence of other factors that may influence metal deposition to sediments in lakes in the region, including variation in sediment composition and grain size, deep-water oxygen concentration, supply from surrounding wetlands, permafrost, and local surficial geology. However, these factors are unlikely to explain the systematic stratigraphic patterns in metal concentrations with respect to distance and wind direction.

5. Conclusions

Collection and analysis of lake sediment cores along two transects were used to identify the record of near- and far-field deposition of metals from Giant and Con mine emissions in the dominant (NW) and non-dominant (NE) wind directions. Enrichment in arsenic and antimony in lake sediment cores during, and shortly after the 1950s, ranging from considerable to severe, demonstrate that emissions from Giant and Con mines were dispersed at least as far as 80 km in the NW and 40 km in the NE. Concentrations of these metals (as well as lead) decreased with distance from Giant Mine and are in agreement with existing literature on mining impacts in the near-field region (Hocking et al. 1978, Wagemann et al.1978, Palmer et al. 2015, Jamieson et al. 2017). However, comparison of lakes in the NE to lakes in the NW at the same distance revealed that the amount of excess arsenic was at least twenty times that of NE20 at NW20, and at least twice that of NE40 at NW40. Given the quantity of excess arsenic and antimony found at lakes NW80 (As: 12 mg/m^2, Sb: 2 mg/m^2) and NE40 (As: 46 mg/m^2, Sb: 3 mg/m^2), located farthest from the

mine along each transect, pollution from Giant and Con mines is unlikely to be limited to the NW or NE and is expected to be present in all wind directions at distances beyond those explored here.

Stratigraphic profiles of arsenic, antimony, and lead at lakes in the NW near-field region suggest enriched metal concentrations found closest to the sediment surface are likely sourced from legacy stores in the surrounding terrestrial environment and lake sediments, and that supply of metal pollutants remains ongoing. Lakes located farther away (NW far-field) and in the non-dominant wind direction (NE), in contrast, have exhausted their lesser supply of terrestrial legacy metals and, in turn allowed the period of maximum emission release in the 1950s to become well-preserved in the lake stratigraphic records. As a result, legacy pollution continues to affect lakes at present in the near-field region where terrestrial and lake sediment sources of legacy metals are more abundant.

The paleolimnological records were instrumental to furthering knowledge of the spatial footprint of mining emissions in this region. Results suggest that future research should aim to characterize terrestrial stores of legacy metals to better understand processes governing the movement of legacy metals from terrestrial to aquatic systems. Confounding impacts from late 20th century climate warming, such as changes in precipitation and wildfire frequency, may accelerate transport of legacy metals and warrant further study (Pelletier et al. 2020b). Systematic collection of lake sediment cores along transects and their analysis may prove fruitful elsewhere to delineate environmental impact in locations where there is an absence of real-time monitoring of point-source emission transport and deposition.

Acknowledgments

Funding for this research was provided by a Global Water Futures grant (Sub-Arctic Metal Mobility Study) to BBW, JJV, RIH and RMC, the Northern Scientific Training Program, the Polar Continental Shelf Program, and an NSERC Alexander Graham Bell Canada Graduate Scholarship awarded to Izabela Jasiak. Authors thank Mackenzie Schultz, Caitlin Dermott, and Tanner Owca at Wilfrid Laurier University, Jennifer Hickman and Casey Beel at the Government of Northwest Territories, and Mia Stratton at University of Waterloo for assistance with field work and sample processing.

References

Abraham, J., Dowling, K., & Florentine, S. (2017). Risk of post-fire metal mobilization into surface water resources: A review. *Science of the Total Environment*¸ 599-600, 1740-1755.

Appleby, P.G. (2001). Chronostratigraphic techniques in recent sediments. In: W.M. Last, J.P. Smol (eds) *Tracking environmental change using lake sediments: Developments in Paleoenvironmental Research*, vol 1. Springer, Dordrecht, 171-203.

Audette, Y., Smith, D.S., Parsons, C.T., Chen, W., Rezanezhad, F. & Van Capellen, P. (2020). Phosphorus binding to soil organic matter via ternary complexes with calcium. *Chemosphere*, 260, 127624.

Bacardit, M., Krachler, M., & Camarero, L. (2012). Whole-catchment inventories of trace metals in soils and sediments in mountain lake catchments in the Central Pyrenees: apportioning the anthropogenic and natural contributions. *Geochimica et Cosmochimica Acta*, 82, 52-67.

Binford, M.W. (1990). Calculation and uncertainty analysis of ^{210}Pb dates for PIRLA project lake sediment cores. *Journal of Paleolimnology*, 3, 253-267.

Birch, G.F. (2017). Determination of sediment metal background concentrations and enrichment in marine environments – a critical review. *Science of the Total Environment*, 580, 813-831.

Boyle, R.W. (1960). The geology, geochemistry and origin of gold deposits of the Yellowknife District. Geology Survey of Canada Memoir 310, Department of Mines and Technical Surveys, Ottawa, Ontario, Canada. 193 p.

Boyle, D., Brix, K.V., Amlund, H., Lundebye, A.K., Hogstrand, C., & Bury, N.R. (2008). Natural arsenic contaminated diets perturb reproduction in fish. *Environmental Science and Technology*, 42, 5354-5360.

Bromstad, M. J., Wrye, L.A., & Jamieson, H.E. (2017). The characterization, mobility, and persistence of roaster-derived arsenic in soils at Giant Mine, NWT. *Applied Geochemistry*, 82, 102-118.

Cai, Y., Zhang, H., Yuan, G., & Li, F. (2017). Sources, speciation and transformation of arsenic in the gold mining impacted Jiehe River, China. *Applied Geochemistry*, 84, 254-261.

Canadian Council of Ministers of the Environment. 1999a. Canadian sediment quality guidelines for the protection of aquatic life: Arsenic. In: Canadian environmental quality guidelines, 1999, Canadian Council of Ministers of the Environment, Winnipeg.

Canadian Council of Ministers of the Environment. 1999b. Canadian sediment quality guidelines for the protection of aquatic life: Lead. In: Canadian environmental quality guidelines, 1999, Canadian Council of Ministers of the Environment, Winnipeg.

Canadian Council of Ministers of the Environment. (2001). Canadian Water Quality Guidelines for the Protection of Aquatic Life: Arsenic. 2nd edition. In: Canadian environmental quality guidelines, 1999, Canadian Council of Ministers of the Environment, Winnipeg.

Cheney, C.L., Eccles, K.M., Kimpe, L.E., Thienpont, J.R., Korosi, J.B., & Blais, J.M. (2020). Determining the effects of past gold mining using a sediment paleotoxicity model. *Science of the Total Environment*, 718, 137308.

Chetelat, J., Amyot, M., Muir, D., Black, J., Richardson, M., Evans, M., & Palmer, M. (2017). Arsenic, antimony, and metal concentrations in water and sediment of Yellowknife Bay. Northwest Territories Geological Survey, NWT Open File 2017-05, 40 p.

Chetelat, J., Cott, P.A., Rosabal, M., Houben, A., McClelland, C., Belle Rose, E., & Amyot, M. (2019). Arsenic bioaccumulation in subarctic fishes of a mine-impacted bay on Great Slave Lake, Northwest Territories, Canada. *PLoS One*, 14, e0221361.

Cott, P.A., Zajdlik, B.A., Palmer, M.J., & McPherson, M.D. (2016). Arsenic and mercury in lake whitefish and burbot near the abandoned Giant Mine on Great Slave Lake. *Journal of Great Lakes Research*, 42, 223-232.

Couture, R.M., Gobeil, C., & Tessier, A. (2008). Chronology of atmospheric deposition of arsenic inferred from reconstructed sedimentary records. *Environmental Science and Technology*, 42, 6508-6513.

Couture, R.M., Gobeil, C., & Tessier, A. (2010). Arsenic, iron, and sulfur co-diagenesis in lake sediments. *Geochimica et Cosmochimica Acta*, 74, 1238-1255.

Ecosystem Classification Group. (2008). Ecological Regions of the Northwest Territories –Taiga Shield. Department of Environment and Natural Resources, Government of the Northwest Territories, Yellowknife, NT, Canada.

Erickson, R.J., Mount, D.R., Highland, T.L., Hockett, J.R., Leonard, E.N., Mattson, V.R., Dawson, T.D., & Lott, K.G. (2010). Effects of copper, cadmium, lead, and arsenic in a live diet on juvenile fish growth. *Canadian Journal of Fisheries and Aquatic Sciences*, 67, 1816-1826.

Fawcett, S.E., Jamieson, H.E., Nordstrom, D.K., & Blaine McCleskey, R. (2015). Arsenic and antimony geochemistry of mine wastes, associated waters and sediments at the Giant Mine, Yellowknife, Northwest Territories, Canada. *Applied Geochemistry*, 62, 3-17.

Fuller, C.C., van Geen, A., Baskaran, M., & Anima, R.J. (1999). Sediment chronology in San Francisco Bay, California, defined by ^{210}210, ^{234}Th, ^{137}Cs, and ^{239,240}Pu. *Marine Chemistry*, 64, 7-27.

Gallon, C., Tessier, A., Gobeil, C., & Alfaro-De La Torre, C. (2004). Modeling diagenesis of lead in sediments of a Canadian Shield lake. *Geochimica et Cosmochimica Acta*, 68, 3531-3545.

Galloway, J.M., Sanei, H, Patterson, R.T., Mosstajiri, T., Hadlari, T., & Falck, H. (2012). Total arsenic concentrations of lake sediments near the city of Yellowknife, Northwest Territories. Geological Survey of Canada, Open File 7037, 47 p.

Galloway, J.M., Palmer, M., Jamieson, H.E., Patterson, R.T., Nasser, N, Falck, H., Macumber, A.L., Goldsmith, S.A., Sanei, H., Normandeau, P., Hadlari, T., Roe, H.M., Neville, L.A., & Lemay, D. (2015). Geochemistry of lakes across ecozones in the Northwest Territories and implications for the distribution of arsenic in the Yellowknife region. Part 1: Sediments, Geological Survey of Canada, Open File 7908, 1.

Galloway, J.M., Swindles, G.T., Jamieson, H.E., Palmer, M., Parsons, M.B., Sanei, H., Macumber, A.I., Patterson, R.T., & Falck, H. (2018). Organic matter control on the distribution of arsenic in lake sediments impacted by ~65 years of gold ore processing in subarctic Canada. *Science of the Total Environment*, 622-623, 1668-1679.

Gawel, J.E., Asplund, J.A., Burdick, S., Miller, M., Peterson, S.M., Tollefson, A., & Ziegler, K. (2014). Arsenic and lead distribution and mobility in lake sediments in the south-central Puget Sound watershed: The long-term impact of a metal smelter in Ruston, Washington, USA. *Science of the Total Environment*, 472, 530-537.

Giesler, R., Clemmensen, K.E., Wardle, D.A., Klaminder, J., & Bindler, R. (2017). Boreal forests sequester large amounts of mercury over millennial time scales in the absence of wildfire. *Environmental Science and Technology*, 51, 2621-2627.

Gomes, F.D.C., Godoy, J.M., Godoy, M.L.D.P., de Carvalho Z.L., Lopes, R.T., Sanchez-Cabeza, J.A., de Lacerda, L.D., & Wasserman, J.C. (2009). Metal concentrations, fluxes, inventories, and chronologies in sediment from Sepetiba and Ribeira Bays: A comparative study. *Marine Pollution Bulletin*, 4-7, 123-133.

Government of Canada. (2014a). History of Giant Mine, Indigenous and Northern Affairs Canada.

Government of Canada. (2014b). Giant Mine historical timeline, Indigenous and Northern Affairs Canada.

Government of Canada (2019). Canadian Climate Normals: Yellowknife, Northwest Territories, Environment and Natural Resources.

Government of Northwest Territories. (n.d.). Concluding and implementing land claim and self government agreements: Tłı̨chǫ, Executive and Indigenous Affairs. https://www.eia.gov.nt.ca/en/priorities/concluding-and-implementing-land-claim-and-self-government-agreements/tlicho (Accessed June 9, 221).

Government of Northwest Territories. (1993). An inventory of atmosphere emissions from the Royal Oak Giant Yellowknife Mine. Department of Renewable Resources.

Government of Northwest Territories. (2016). A guide to the mineral deposits of the Northwest Territories. Department of Industry, Tourism, and Investment. Online resource.

Grosbois, C., Courtin-Nomade, A., Robin, E., Bril, H., Tamura, N., Schäfer, J., & Blanc, G. (2011). Fate of arsenic-bearing phases during the suspended transport in a gold mining district (Isle river Basin, France). *Science of The Total Environment*, 409, 4986-4999.

Han, F.X., Su, Y., Monts, D.L., Plodinec, M.J., Banin, A., & Triplett, G.E. (2003). Assessment of global industrial-age anthropogenic arsenic contamination. *Naturwissenschasften*, 90, 395-401.

Heiri, O., Lotter, A.F., & Lemcke, G. (2001). Loss on ignition as a method for estimating organic and carbonate content in sediments: reproducibility and comparability of results. *Journal of Paleolimnology*, 25, 101-110.

Herath, I., Vithanage, J., & Bundschuh, J. (2017). Antimony as a global dilemma: geochemistry, mobility, fate, and transport. *Environmental Pollution*, 223, 545-559.

Hocking, D., Kuchar, P., Plambeck, J.A., & Smith, R.A. (1978). The impact of gold smelter emissions on vegetation and soils of a sub-arctic forest-tundra transition ecosystem. *Journal of the Air Pollution Control Association*, 28, 133-137.

Houben, A. J., D'Onofrio, R., Kokelj, S. V., & Blais, J. M. (2016). Factors affecting elevated arsenic and methyl mercury concentrations in small shield lakes surrounding gold mines near the Yellowknife, NT, (Canada) region. *Plos One*, 11, e0150960.

Hutchinson, T. C., Aufreiter, S., & Hancock, R. G. (1982). Arsenic pollution in the Yellowknife Area from gold smelter activities. *Journal of Radioanalytical Chemistry*, 71, 59-73.

Indian and Northern Affairs Canada. (2007). Giant Mine Remediation Plan. Giant Mine Remediation Project Team, Prepared by SRK Consulting Inc. and SENES Consultants Limited, Department of Indian Affairs and Northern Development, Yellowknife, Northwest Territories.

Jamieson, H.E. (2014). The legacy of arsenic contamination from mining and processing refractory gold ore at Giant Mine, Yellowknife, Northwest Territories, Canada. *Reviews in Mineralogy & Geochemistry*, 79, 533-551.

Jamieson, H.E., Maitland, K.M., Oliver, J.T., & Palmer, M.J. (2017). Regional distribution of arsenic in near-surface soils in the Yellowknife area. Northwest Territories Geological Survey, NWT Open File 2017-03, 28 p.

Kay, M.L., Wiklund, J.A., Remmer, C.R., Owca, T.J., Klemt, W.H., Neary, L.K., Brown, K., MacDonald, E., Thomson, K., Vucic, J.M., Wesenberg, K., Hall, R.I., & Wolfe, B.B. (2020). Evaluating temporal patterns of metals concentrations in floodplain lakes of the Athabasca Delta (Canada) relative to pre-industrial baselines. *Science of the Total Environment*, 704, 135309.

Keshavarzi, B., Moore, F., Rastmanesh, F., & Kermani, M. (2012). Arsenic in the Muteh gold mining district, Isfahan, Iran. *Environmental Earth Sciences*, 67, 959-970.

Kinimo, K. C., Yao, K. M., Marcotte, S., Kouassi, N. L., & Trokourey, A. (2018). Distribution trends and ecological risks of arsenic and trace metals in wetland sediments around gold mining activities in central-southern and southeastern Côte dIvoire. *Journal of Geochemical Exploration*, 190, 265-280.

Klemt, W. H., Kay, M.L., Wiklund, J.A., Wolfe, B.B, & Hall, R.I. (2020). Assessment of vanadium and nickel enrichment in Lower Athabasca River floodplain lake sediment within the Athabasca Oil Sands Region (Canada). *Environmental Pollution*, 265, 114920.

Leclerc, E., Venkiteswaran, J.J., Jasiak, I., Telford, J.V., Wolfe, B.B., Hall, R.I., Schultz, M.D.J., & Couture, R.M.C. Quantifying arsenic post-depositional mobility in lake sediments impacted by gold ore roasting in sub-arctic Canada using inverse diagenetic modelling. *Environmental Pollution*, in review.

MacDonald, L. A., Wiklund, J. A., Elmes, M. C., Wolfe, B. B., & Hall, R. I. (2016). Paleolimnological assessment of riverine and atmospheric pathways and sources of metal deposition at a floodplain lake (Slave River Delta, Northwest Territories, Canada). *Science of the Total Environment*, 544, 811-823.

Martin, A.J., & Pederson, T.F. (2002). Seasonal and interannual mobility of arsenic in a lake impacted by metal mining. *Environmental Science and Technology*, 36, 1516-1523.

Miller, C.B., Parsons, M.B., Jamieson, H.E., Swindles, G.T., Nasser, N.A., & Galloway, J.M. (2019). Lake-specific controls on the long-term stability of mining-related legacy arsenic contamination and geochemical baselines in a changing northern environment, Tundra Mine, Northwest Territories, Canada. *Applied Geochemistry*, 109, 104403.

Morra, J.M., Carter, M.M., Rember W.C., & Kaste, J.M. (2015). Reconstructing the history of mining and remediation in the Coeur d'Alene, Idaho Mining District using lake sediments. *Chemosphere*, 134, 319-327.

Mudroch, A., & Clair, T. (1986). Transport of arsenic and mercury from gold mining activities through an aquatic system. *Science of the Total Environment*, 57, 205-216.

Mudroch, A., Joshi, S.R., Sutherland, D., Mudroch, P., & Dickson, K.M. (1989). Geochemistry of sediments in the back bay and Yellowknife Bay of the Great Slave lake. *Environmental Geology and Water Sciences*, 14, 35-42.

Muir, D. C. G., Wang, X., Yang, F., Nguyen, N., Jackson, T. A., Evans, M. S., Douglas, M., Köck, G., Lamoureux, S., Pienitz, R., Smol, J. P., Vincent, W. F., & Dastoor, A. (2009). Spatial trends and historical deposition of mercury in Eastern and Northern Canada inferred from lake sediment cores. *Environmental Science and Technology*, 43, 4802-4809.

Ng, J., & Gomez-Caminero, A. (2001). Arsenic and arsenic compounds (2nd edition). World Health Organization.

Olid, C., Garcia-Orellana, J., Martinez-Cortizas, A., Masque, P., Peiteado-Varela, E., & Sanchez-Cabeza, J.A. (2010). Multiple site study of recent atmospheric metal deposition (Pb, Zn, Cu) deposition in the NW Iberian Peninsula using peat cores. *Science of the Total Environment*, 408, 5540-5549.

Outridge, P.M. & Wang, F. (2015). The stability of metal profiles in freshwater and marine sediments. In J.M. Blais, M.R. Rosen, J.P. Smol. (eds). Environmental Contaminants: Using natural archives to track sources and long-term trends of pollution. *Developments in Paleoenvironmental Research*, vol. 18, Springer, Netherlands, 35-60.

Palmer, M.J., Galloway, J.M., Jamieson, H.E., Patterson, R.T., Falck, H, and Kokelj, S.V. (2015). The concentration of arsenic in lake waters of the Yellowknife area, Northwest Territories Geological Survey, NWT Open File 2015-06. 25 p.

Palmer, M.J., Chetelat, J., Richardson, M., Jamieson, H.E., & Galloway, J.M. (2019). Seasonal variation of arsenic and antimony in surface waters of small subarctic lakes impacted by legacy mining pollution near Yellowknife, NT, Canada. *Science of the Total Environment*, 684, 326-339.

Palmer, M.J., Chételat, J., Jamieson, H.E., Richardson, M. and Amyot, M. (2021), Hydrologic control on winter dissolved oxygen mediates arsenic cycling in a small subarctic lake. *Limnology and Oceanography*, 66, S30-S46. https://doi.org/10.1002/lno.11556

Pelletier, N., Chetelat, J., Cousens, B., Zhang, S., Stephner, D., Muir, D.C.G., & Vermaire, J.C. (2020). Lead contamination from gold mining in Yellowknife Bay (Northwest Territories), reconstructed using stable lead isotopes. *Environmental Pollution*, 259, 113888.

Pelletier, N., Chetelat, J., Blarquez, O., & Vermaire, J.C. (2020b). Paleolimnological assessment of wildfire-derived atmospheric deposition of trace metal(loid)s and major ions to subarctic lakes (Northwest Territories, Canada). *Journal of Geophysical Research: Biogeosciences*, 125, 1-14.

Peter, S.A., & Wozniak, J.A. (2001). Lead analysis of sediment cores from seven Connecticut lakes. *Journal of Paleolimnology*, 26, 1-10.

de Rosemond, S., Xie, Q., & Liber, K. (2008). Arsenic concentration and speciation in five freshwater fish species from Back Bay near Yellowknife, NT, Canada. *Environmental Monitoring and Assessment*, 147, 199-210.

Sandlos, J., & Keeling, A. (2012). Claiming the New North: Development and Colonialism at the Pine Point Mine, Northwest Territories, Canada. Environment and History, 18, 5-34.

Schelske, C. L., Peplow, A., Brenner, M., and Spencer, C. N. (1994). Low-background gamma counting: applications for ^{210}Pb dating of sediments. *Journal of Paleolimnology*, 10, 115-128.

Schuh, C. E., Jamieson, H. E., Palmer, M. J., & Martin, A. J. (2018). Solid-phase speciation and post-depositional mobility of arsenic in lake sediments impacted by ore roasting at legacy gold mines in the Yellowknife area, Northwest Territories, Canada. *Applied Geochemistry*, 91, 208-220.

Schuh, C.E., Jamieson, H. E., Palmer, M.J., Martin, A. J., & Blais, J.M. (2019). Controls governing the spatial distribution of sediment arsenic concentrations and solid-phase speciation in a lake impacted by legacy mining pollution. *Science of the Total Environment*, 654, 563-575.

Sharma, V.K., & Sohn, M. (2009). Aquatic arsenic: toxicity, speciation, transformations, and remediation. *Environment International*, 35, 743-59.

Sivarajah, B., Korosi, J.B., Blais, J.M., & Smol, J.P. (2019). Multiple environmental variables influence diatom assemblages across an arsenic gradient in 33 subarctic lakes near abandoned gold mines. *Hydrobiologia*, 841, 133-151.

Sivarajah, B., Cheney, C.L., Perrett, M., Kimpe, L.E., Blais, J.M., & Smol, J.P. (2020). Regional gold mining activities and recent climate warming alter diatom assemblages in deep sub-Arctic lakes. *Polar Biology*, 43, 305-317.

Smedley, P., & Kinniburgh, D. (2002). A review of the source, behaviour and distribution of arsenic in natural waters. *Applied Geochemistry*, 17, 517-568.

Smol, J.P. (2008). Pollution of lakes and rivers: a paleoenvironmental perspective, (2nd ed.), Blackwell Pub.

SRK Consulting Engineers and Scientists. (2002). Final Report: Giant Mine Arsenic Trioxide Management Alternatives, submitted to Department of Indian and Northern Affairs Canada, Yellowknife, NT, p.140.

Stubley, M.P. & Irwin, D. (2019). Bedrock geology of the Slave Craton, Northwest Territories and Nunavut. Northwest Territories Geological Survey, NWT Open File 2019-01. ESRI and Adobe digital files.

Tenkouano, G-T., Cumming, B.F., & Jamieson, H.E. (2019). Geochemical and ecological changes within Moira Lake (Ontario, Canada): a legacy of industrial contamination and remediation. *Environmental Pollution*, 247, 980-988.

Thevenon, F., Graham, N.D., Chiaradia, M., Chiaradia, M., Arpagaus, P., Wildi, W., & Pote, J. (2011). Local to regional scale industrial heavy metal pollution recorded in sediments of large freshwater lakes in central Europe (lakes Geneva and Lucerne) over the last centuries. *Science of the Total Environment*, 412-413, 239-247.

Thienpont, J. R., Korosi, J. B., Hargan, K. E., Williams, T., Eickmeyer, D. C., Kimpe, L. E., Palmer, M.J., Smol, J.P., & Blais, J. M. (2016). Multi-trophic level response to extreme metal contamination from gold mining in a subarctic lake. *Proceedings of the Royal Society B: Biological Sciences*, 283, 20161125.

Tian, H., Zhou, J., Zhu, C., Zhao, D., Gao, J., Hao, M.H., Liu, K., Wang, K., & Hua, S. (2014). A comprehensive global inventory of atmospheric antimony emissions from anthropogenic activities, 1995-2010. *Environmental Science and Technology*, 48, 10235-10241.

Turekian, K.K., & Wedepohl, K.H. (1961). Distribution of the elements in some major units of the earth's crust. *Geological Society of America Bulletin*, 72, 175-192.

Van Den Berghe, M., Jamieson, H.E., & Palmer, M.J. (2018). Arsenic mobility and characterization in lakes impacted by gold ore roasting, Yellowknife, NWT, Canada. *Environmental Pollution*, 234, 630-641.

Wagemann, R., Snow, N. B., Rosenberg, D. M., & Lutz, A. (1978). Arsenic in sediments, water and aquatic biota from lakes in the vicinity of Yellowknife, Northwest Territories, Canada. *Archives of Environmental Contamination and Toxicology*, 7, 169-191.

Wai, K.M., Wu, S., Li, X., Jaffe, D.A., & Perry, K.D. (2016). Global atmospheric transport and source-receptor relationships for arsenic. *Environmental Science and Technology*, 50, 3714-3720.

Walker, S. R., Jamieson, H. E., Lanzirotti, A., Andrade, C. F., & Hall, G. E. (2005). The speciation of arsenic in iron oxides in mine wastes from the Giant gold mine, N.W.T.: application of synchrotron micro-xrd and micro-xanes at the grain scale. *The Canadian Mineralogist*, 43, 1205-1224.

Walker, S.R., Jamieson, H.E., Lanzirotti, A., Hall, G.E.M., & Peterson, R.C. (2015). The effect of ore roasting on arsenic oxidation state and solid phase speciation in gold mine tailings. *Geochemistry: Exploration, Environment, Analysis*, 15. 273-291.

Wang, X., Thompson, D.K., Marshall, G.A., Tymstra, C., Carr, R., & Flannigan, M.D. (2015). Increasing frequency of extreme fire weather in Canada with climate change. *Climate Change*, 130, 573-586.

Whitmore, T.J., Reidinger-Whitmore, M.A., Smoak, J.M., Kolasa, K.V., Goddard, E.A., & Bindler, R. (2008). Arsenic contamination of lake sediments in Florida: evidence of herbicide mobility from watershed soils. *Journal of Paleolimnology*, 40, 869-884.

Wiklund, J.A., Hall, R.I., Wolfe, B.B., Edwards, T.W.D., Farwell, A.J. & Dixon, D.G. (2012). Has Alberta oil sands development increased far-field delivery of airborne contaminants to the Peace-Athabasca Delta? *Science of the Total Environment*, 433, 379-382.

Wiklund, J.A., Kirk, J.L., Muir, D.C.G., Evans, M., Yang, F., Keating, J., & Parsons, M.T. (2017). Anthropogenic mercury deposition in Flin Flon Manitoba and the Experimental Lakes Area Ontario (Canada): A multi-lake sediment core reconstruction. *Science of the Total Environment*, 586, 685-695.

Wiklund, J.A., Kirk, J.L., Muir, D.C.G., Gleason, A., Carrier, J., & Yang, F. (2020). Atmospheric trace metal deposition to remote Northwest Ontario Canada: Anthropogenic fluxes and inventories from 1860 to 2010. *Science of the Total Environment*, 749, 142276.

Wong, C.H., Sanders, G., Engstrom, D.R., Long, D.T., Swackhamer, D.L., & Eisenreich, S.J. (1995). Accumulation, inventory, and diagenesis of chlorinated hydrocarbons in Lake Ontario sediments. *Environmental Science and Technology*, 29, 2661-2672.

Table 1: Select basin characteristics of study lakes to the northwest and northeast of Giant Mine. Lakes are grouped into Near-field, Far-field, and Northeast.

Lake	Coordinates (Lat., Long.)	Distance from Giant Mine (km)	Size (km^2)	Depth (m)
Near-field				
NW10	62.552889, -114.52625	10.5	0.21	1.5
NW20	62.608333, -114.605278	17.8	1.12	4.0
NW30	62.672278, -114.812028	29.8	0.08	3.0
NW40	62.738889, -114.958333	40.6	2.60	8.0
Far-field				
NW50	62.825556, -115.009639	49.6	2.72	24.0
NW60	62.834694, -115.158417	55.7	1.56	3.5
NW70	62.951111, -115.367222	72.5	0.44	5.0
NW80	63.002056, -115.444528	79.0	0.08	7.0
Northeast				
NE20	62.598334, -114.017256	20.9	1.05	10.6
NE40	62.705842, -113.682029	41.2	0.20	3.0

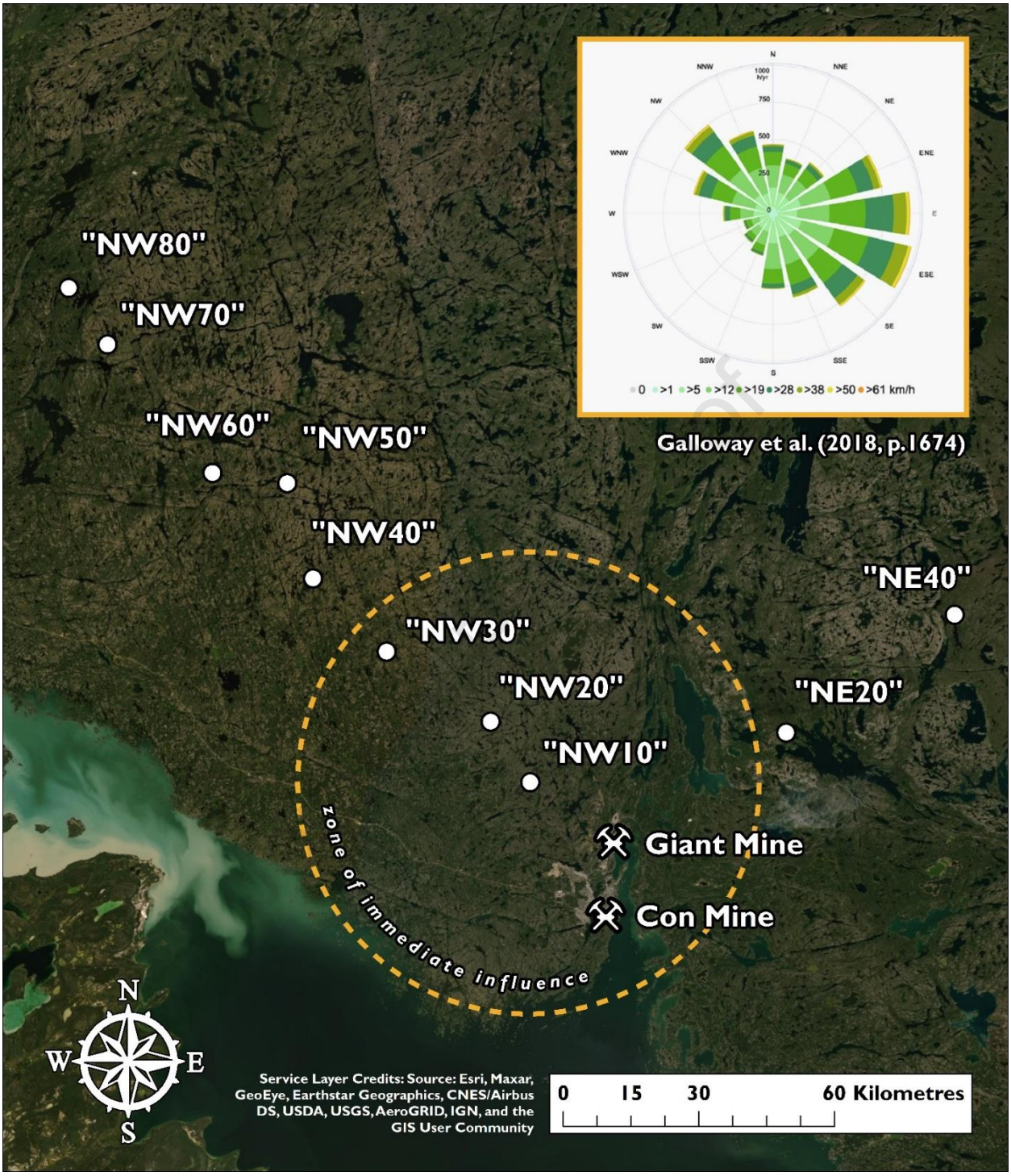

Figure 1: Map showing locations of the study lakes relative to the 'zone of immediate influence' of Giant Mine emissions identified by Palmer et al. (2015). Top-right inset provides a wind rose illustrating winds that dominantly blow from southeast to the northwest in this region (Galloway et al. 2018, p.1674).

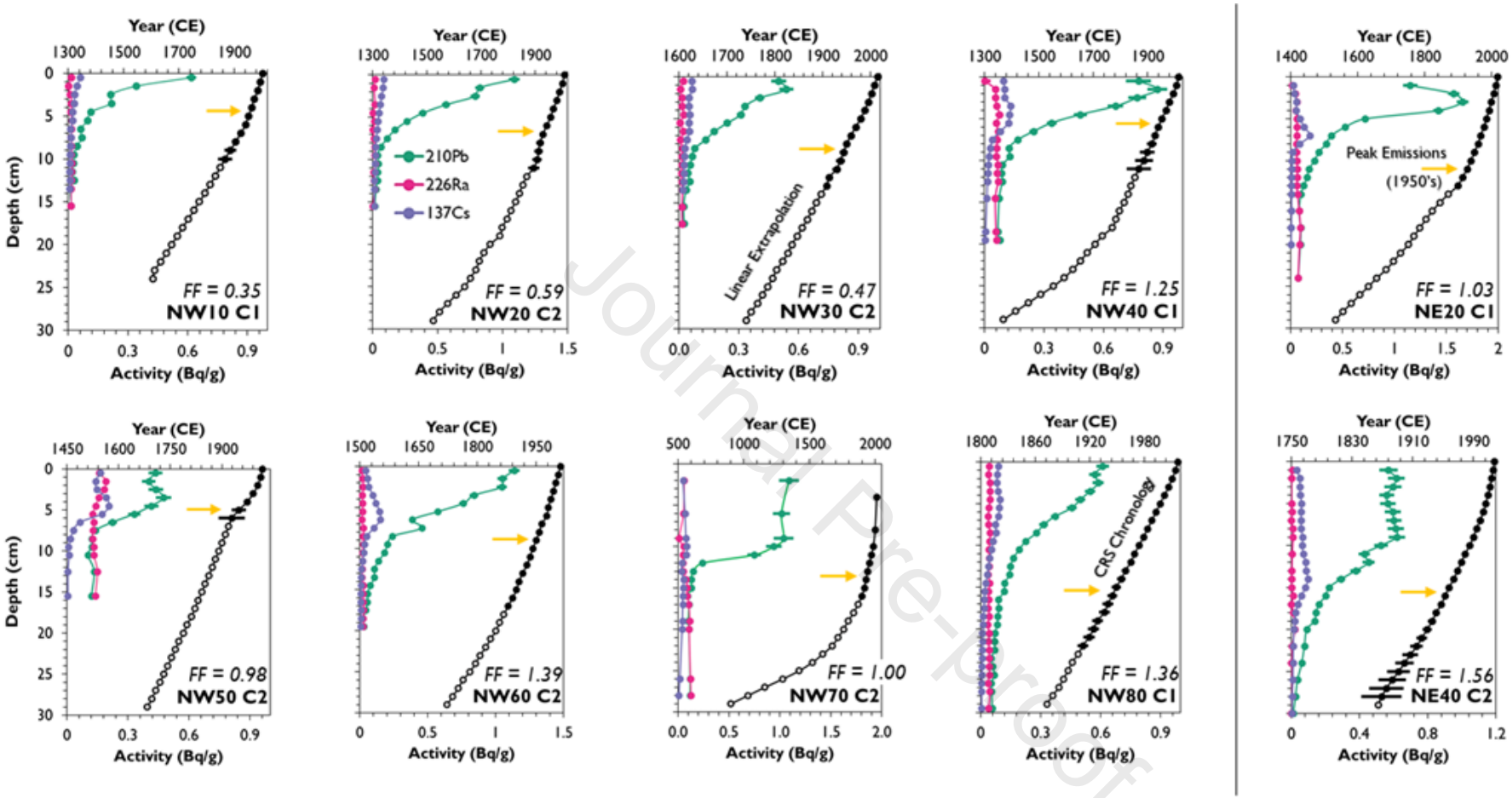

Figure 2: Profiles of ^{210}Pb, ^{226}Ra, and ^{137}Cs activity shown stratigraphically for lakes along the northwest (left) and northeast (right) transects. Only the upper 30 intervals at each lake are shown here. In black, the CRS-based age model depicts the corresponding year for each sediment interval where black horizontal bars on either side represent the associated error (±2 standard deviation units). Extrapolations of the CRS chronology are denoted by white filled data points while the 1950s, representing the timing of peak emissions from Giant and Con mines, is shown by the yellow arrow. The focusing factor for each lake as calculated by ^{210}Pb inventories is denoted by "FF" above the lake name.

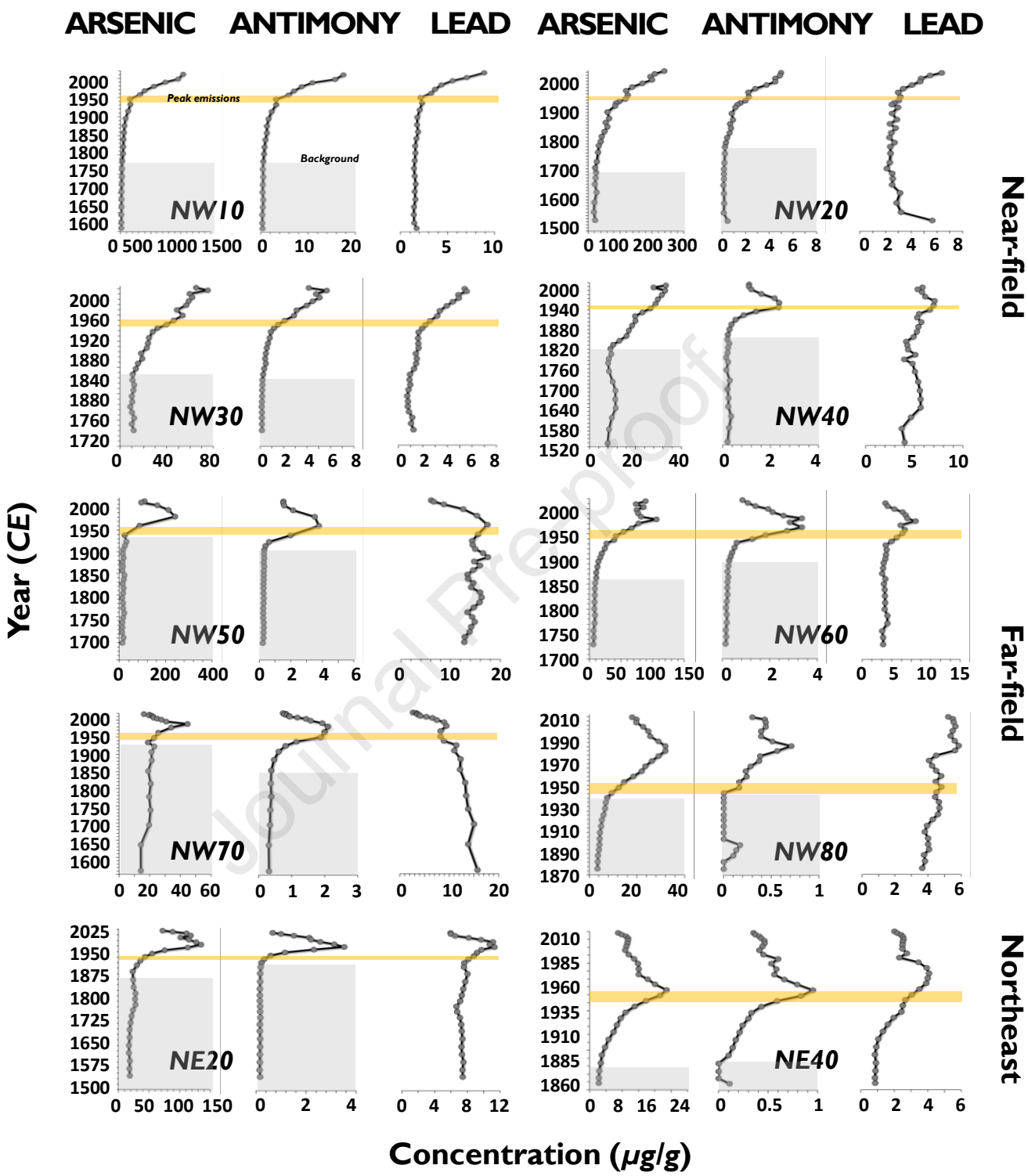

Figure 3: Stratigraphic profiles of arsenic, antimony, and lead concentrations for lakes across the northwest and northeast transects. Results are presented to 1500 CE where available. The period of peak emissions is highlighted in yellow (i.e., 1950s) while the grey shaded areas represent the period identified as background.

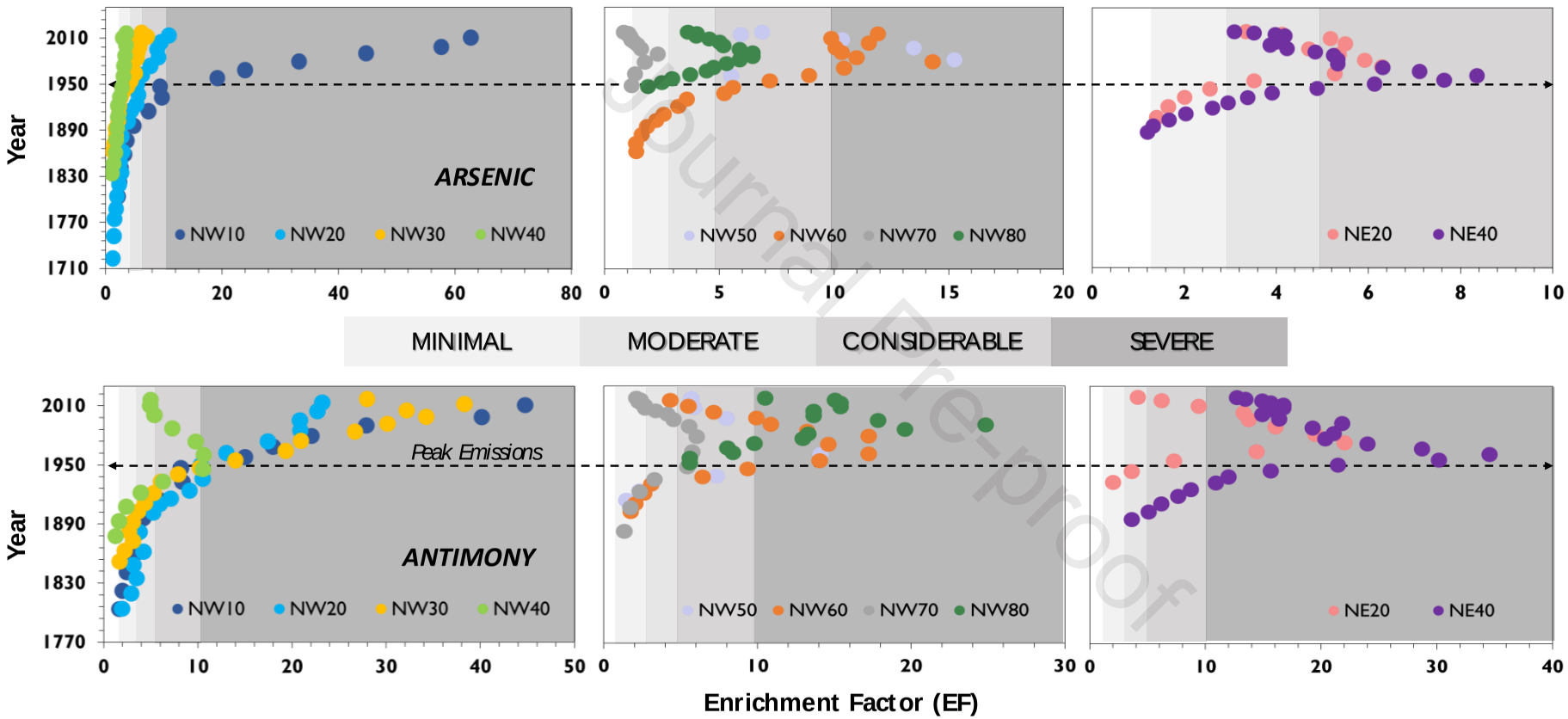

Figure 4: Temporal patterns of Enrichment Factors for arsenic (top) and antimony (bottom) at NW transect near-field (left) and far-field (middle) lakes, and NE transect (right) lakes. Degree of enrichment is shown relative to the categories identified by Birch (2017).

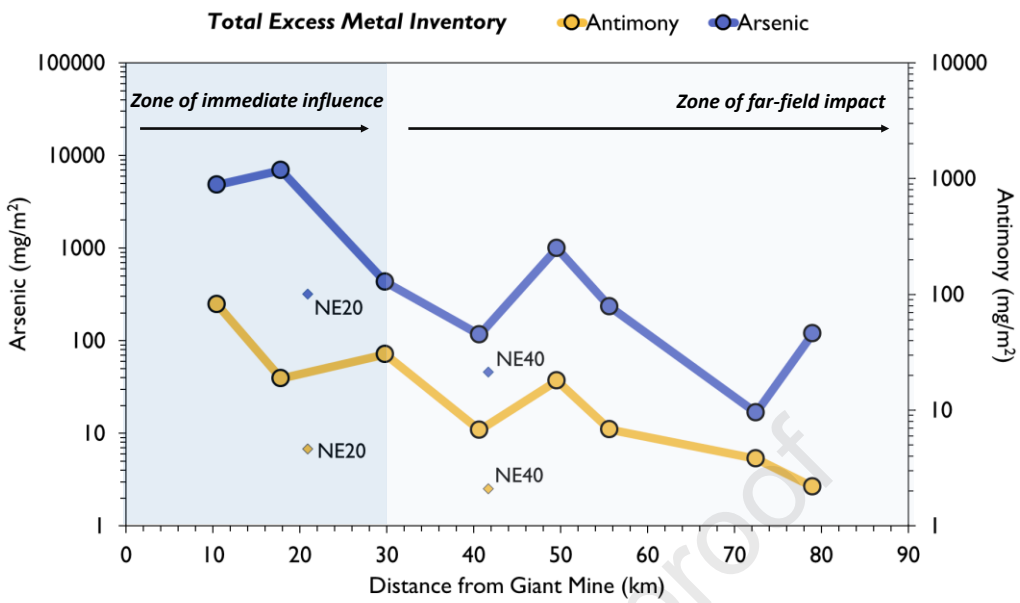

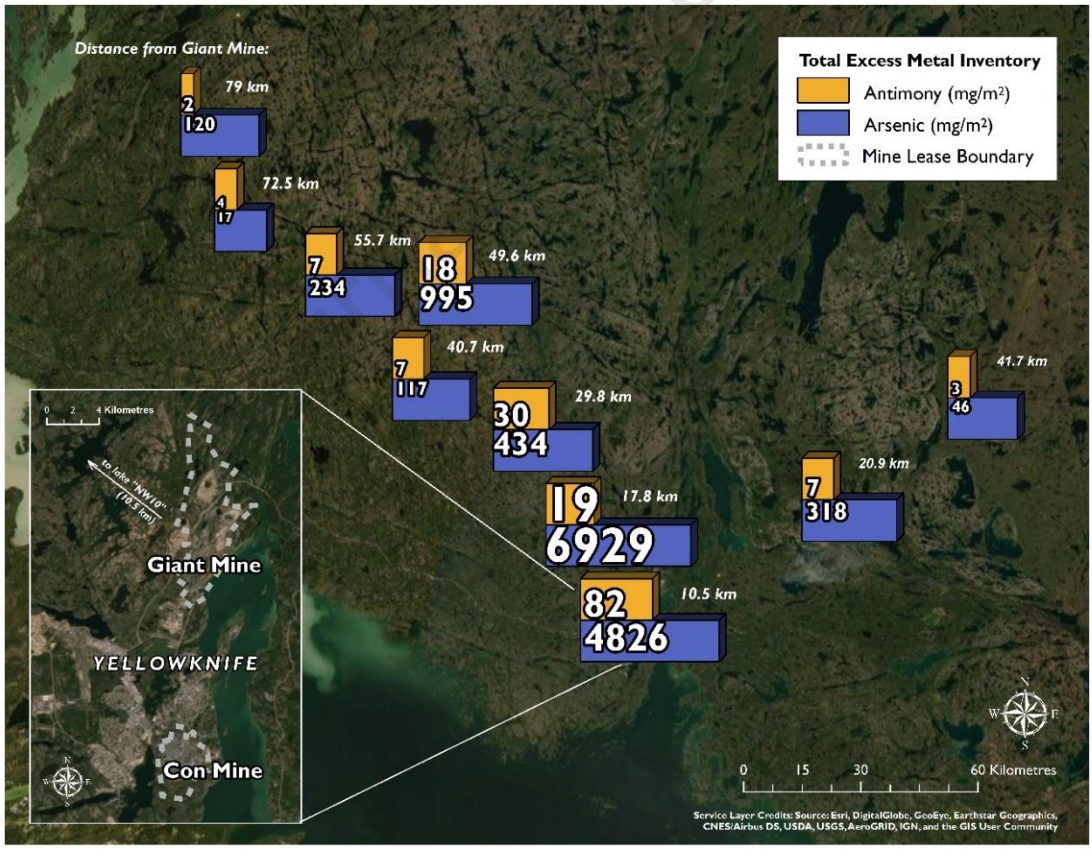

Figure 5: Calculated excess metal inventories for arsenic and antimony at all study lakes. Metal concentrations were focus-factor (FF) corrected and either increased (FF < 1: NW10, NW20, NW30, NW50) or decreased (FF > 1: NW40, NW60, NW70, NW80, NE20, NE40) the estimated excess metal inventory. Top: arsenic and antimony inventories are shown according to distance from Giant Mine. Bottom: metal inventories are shown relative to wind direction.

Highlights

- We analyze metals in sediment cores to track dispersal of legacy mine emissions
- Enrichment of As and Sb evident beyond known 30-km radius pollution zone
- Distance from source and wind direction influenced contaminant dispersal
- Enriched surface sediments within 30 km suggest ongoing delivery of legacy metals

Declaration of interests

X The authors declare that they have no known competing financial interests or personal relationships that could have appeared to influence the work reported in this paper.

☐The authors declare the following financial interests/personal relationships which may be considered as potential competing interests: